Optics Letters

Reduction of zero baseline drift of the Pound–Drever–Hall error signal with a wedged electro-optical crystal for squeezed state generation

Zhixiu Li,[1,3] Weiguang Ma,[2,3] Wenhai Yang,[1,3] Yajun Wang,[1,3] and Yaohui Zheng[1,3,*]

[1]The State Key Laboratory of Quantum Optics and Quantum Optics Devices, Institute of Opto-Electronics, Shanxi University, Taiyuan, Shanxi 030006, China
[2]The State Key Laboratory of Quantum Optics and Quantum Optics Devices, Institute of Laser Spectroscopy, Shanxi University, Taiyuan, Shanxi 030006, China
[3]Collaborative Innovation Center of Extreme Optics, Shanxi University, Taiyuan, Shanxi 030006, China
*Corresponding author: yhzheng@sxu.edu.cn

Received 16 May 2016; revised 14 June 2016; accepted 15 June 2016; posted 20 June 2016 (Doc. ID 265299); published 14 July 2016

We report an electro-optic modulator (EOM) with a wedged MgO: $LiNbO_3$ as the modulation crystal to reduce the zero baseline drift (ZBD) of the Pound–Drever–Hall (PDH) error signal. When the input linear polarization is not along the modulation direction, the wedged design can separate the two orthogonal polarizations in space after the EOM and eliminate the interference between the carrier and the two orthogonal sidebands. Therefore, the residual amplitude modulation (RAM) of phase modulation process caused by the input polarization misalignment and the etalon effect can be significantly reduced. The noise power spectrum of phase-modulated light with wedged crystal EOM is suppressed from −24 to −69 dBm, which is much lower than that with conventional EOM. The peak-to-peak value of the ZBD of the PDH error signal is reduced effectively to +70/−50 ppm during the 10 h, which meets the requirements for stable squeezed light generation.

OCIS codes: (230.4110) Modulators; (120.5060) Phase modulation; (270.6570) Squeezed states; (190.4970) Parametric oscillators and amplifiers.

http://dx.doi.org/10.1364/OL.41.003331

Squeezed state of light is an important resource for many applications, including precision measurement such as gravitational wave detection [1,2] and quantum information processing for continuous variables [3,4]. For the advanced applications of squeezed light, the generation of stable squeezed light is a critical task. A typical method to generate squeezed light is the utilization of a sub-threshold optical parametric oscillator (OPO) [5,6]. The stability of the squeezing factor is mainly limited by the quality of the servo-control system. In an actual schematic of the experiment, at least three servo-control loops are required: OPO cavity length, relative phase between the pump and signal lights, and relative phase between the local oscillator (LO) and the signal light. Frequency detuning from the cavity resonance, equivalent to the rotation of the squeezing angle, will decrease the squeezing degree [7,8]. At the same time, the phase difference with the desired value, which will mix the squeezed and anti-squeezed quadratures, also deteriorates the quantum noise reduction [9–12]. However, it is well known that almost all the electro-optic modulators (EOMs) generate some unwanted residual amplitude modulation (RAM), which results in the systematic zero baseline drift (ZBD) of the Pound–Drever–Hall (PDH) error signal [13–15] and, hence it degrades the cavity- and phase-locking performance and is especially detrimental in the quantum noise stability of the squeezed state.

The ZBD of error signal in the PDH technique [16] originates primarily from two mechanisms: the birefringence of the electro-optic (EO) crystal [17–20] and the etalon effect formed by two parallel end facets of the EO crystal [13]. Compounding matters, these effects are often sensitive to temperature and stress variations, which impede the realization of long-term stable squeezed light [18,21]. It is possible to reduce the ZBD of the PDH error signal originating from birefringence effect with extreme care in aligning the input polarization direction to match the crystal's principal axis. However, the polarization fluctuation of the input beam and inevitable misalignment cannot be thoroughly eliminated. The most effective method of compensating for the effect of the phase difference due to natural birefringence is the employment of an active servo control to change either the modulation voltage or the crystal's temperature [17–20,22–24]. In addition, to sufficiently suppress the spurious etalon effect of the EO crystal, all optical surfaces are tilted slightly off the normal incidence of the laser beam [14]. In an actual squeezed generation system, besides the three servo control loops, any additional control loops to suppress

the ZBD of the PDH error signal will increase not only the system complexity, but also the adjustment difficulty.

In this Letter, a wedged MgO:$LiNbO_3$ crystal is used as the EO crystal. Due to its natural birefringent, except for the EO modulation, the crystal also acts as a polarizer to separate the misaligned polarization light into two beams with the polarizations parallel to the crystal's principal axes in space. One is used as the signal light for the cavity- and phase-locking, and the other is blocked. Amplitude modulation originating from the superposition of the two beams after the EOM is significantly reduced. By comparing with the conventional EOM, the noise power spectrum of phase-modulated light with the wedged EOM can be distinguished suppressed from −24 to −69 dBm. The peak-to-peak value of the ZBD of the PDH error signal is limited to +70/−50 ppm during the 10 h, which is much lower than the value obtained by using the conventional EOM.

An EOM is a device used to modulate the phase of a laser beam, consisting of a birefringence crystal and a pair of electrodes imposing on the crystal along one of the principal axes. Lithium niobate ($LiNbO_3$) with an MgO concentration is one of the most commonly used ferroelectric crystals in EOMs [14,25]. Figure 1 shows the generation principle of RAM and the ZBD of the PDH error signal. The z- and y-axes are the principal axes of the extraordinary and ordinary waves, respectively. The laser propagates along the x-axis; two end faces are perpendicular to the x-axis for the conventional design. A modulation field parallel to the z-axis is applied to the crystal. Under ideal conditions, the laser beam, with the polarization direction parallel to z-axis, passes through the EOM, and there is a pure phase modulation, where the baseline of error signal is under zero offset and is kept as constant.

However, in practice, it is inevitable to have a small polarization noise of laser beam, and axis mismatch between the incident polarized and the principal axes of the EO crystal. Consequently, the laser beam is divided into the ordinary beam and the extraordinary beam in the EO crystal, where these polarization directions are orthogonal. After the EOM, the output of the modulated light includes two orthogonal sets of carriers and two sidebands, all of which are superposed in space. Polarizing optical components downstream will make the orthogonal carriers and the sidebands interfere mutually. The phase delay difference of the two polarization components within the EO crystal destroys the balance of the triplet of phase-modulated light. In addition, imperfect antireflection coatings of the two parallel end facets causes a fringelike variation in intensity associating with the change of temperature and stress [13,26]. All of these mechanisms result in the ZBD of the PDH error signal.

According to the descriptions above, the separation of the two polarization components in space is a simple and effective method. To realize this purpose, distinguishing from the conventional EO crystal with two parallel end facets is proposed, where one of the end faces is wedged by 4° against the z-axis of the crystal (shown in Fig. 2). The basic working principal of the wedge design is that the deflection angles of the ordinary light and the extraordinary light are different through the wedged facet due to the natural birefringence of the crystal [27,28]. The ordinary wave is separated from the extraordinary wave in space; the ZBD of the PDH error signal originating from birefringence effect can be significantly reduced. It is worth noting that the design also reduces the ZBD of the PDH error signal that results from the etalon effect.

Figure 2 shows the experimental setup for measuring the noise power spectrum of phase-modulated light and the ZBD of the PDH error signal. A homemade single-frequency Nd:YVO_4 laser at 1064 nm is used [29]. An optical isolator (OI1) in front of the laser is used to minimize the backreflections. The linearly polarized beam incident in the EOM is ensured with a purity of better than 1:100000 by using a Glan–Thompson prism (GTP). Another GTP is located after the EOM as a downstream polarizing optical component, which aligns along the propagation direction of the extraordinary wave. The unwanted ordinary light is blocked by a dump in front of the downstream prism. Other additional optical isolators (OI3 and OI4) are placed in front of the photodetector to suppress spurious etalon effects in the optical setup [18]. Two $LiNbO_3$ crystals with conventional and wedged end facets are used as the modulation medium, respectively, which have the same cutting orientation and size. Both EOMs have a modulation index of around 0.1. For the conventional EOM, the RAM level, arising from multipassing fringe effects, depends on the incidence angle of optical beam into the EOM [14]. In the experiment, the incidence angle is adjusted to 1.2° to get the minimum RAM, which compares with the RAM level of the wedged EOM.

A beam splitter is placed in front of the cavity, where its reflected beam is directly coupled into the photodetector (PD1). The output of the beam splitter is fed into an RF spectrum analyzer to measure the noise power spectrum of phase-modulated light. Another photodetector (PD2) reads the

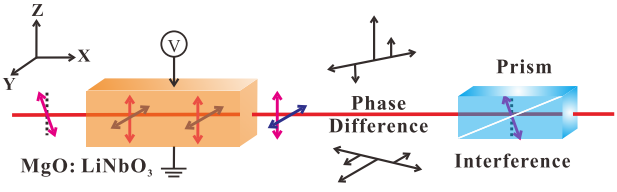

Fig. 1. Generation principle of RAM and the ZBD of the PDH error signal.

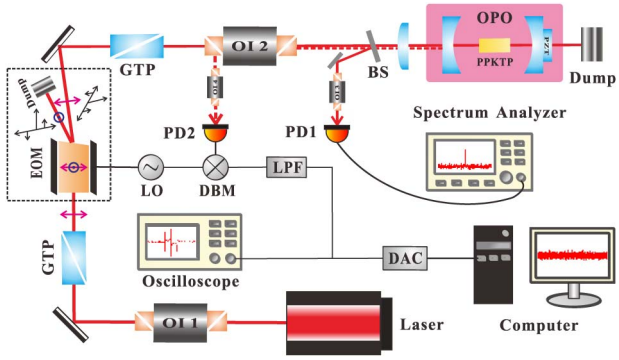

Fig. 2. Experimental setup for measuring the noise power spectrum of phase-modulated light and the ZBD of the PDH error signal. EOM, electro-optic modulator; GTP, Glan–Thompson prism; OI, optical isolator; BS, beam splitter; OPO, optical parametric oscillator; PPKTP, periodically poled $KTiOPO_4$; LO, local oscillator; DBM, doubly balanced mixer; PD, photodetector; LPF, low pass filter; DAC, data acquisition card.

reflected signal of the OPO from the optical isolator (OI2). The RF signal used for frequency modulation acts as a LO to be mixed with the PD2 signal. The phase of the LO is adjusted to give a maximum error signal in the mixer output. When the laser frequency is tuned far from the cavity resonance, the mixer output corresponds to the zero baseline of error signal, which is fed into a NI data acquisition card (DAC) to measure the ZBD of the PDH error signal.

Figure 3 shows the noise power spectra of phase-modulated light signal monitored by PD1 and recorded with the RF spectrum analyzer with conventional and wedged modulation crystals, respectively. When the wedged crystal is used as the modulation medium, the RAM is suppressed by 45 dB, compared with conventional EOM. The remaining RAM is approximately 30 dB higher than the shot noise floor of PD1 at a resolution bandwidth of 100 Hz, and video bandwidth of 10 Hz, which may come from spatial inhomogeneity of the electric field inside the crystal, amplitude fluctuation of the RF power, or frequency fluctuation of the laser [18,23].

To evaluate the long-term stability of zero baseline, we perform a 10 h record of error signal from the mixer recorded by a NI DAC when the laser frequency is far away from the cavity resonance. In the 10 h period, the zero baseline is recorded, which can be converted into a relative fluctuation, with units of ppm, divided by the peak-to-peak value of the error signal. The relative fluctuation can be directly converted into the frequency and phase fluctuation in a definiteness system. Figure 4 compares the time-related zero baseline offset of error signals with the conventional and wedged modulation crystals, respectively. With the former one, the maximum zero baseline offset is about +3500/ – 3400 ppm in 10 h. Replaced by the latter one, the maximum zero baseline offset of error signal is reduced to +70/ – 50 ppm, which is roughly 1/50 of the former. In the experimental setup of squeezed light generation, the ZBD of error signal, originating from the RAM, gives rise to the OPO cavity length and relative phase fluctuations in the vicinity of the resonance point and desired value. These fluctuations drive the squeezing noise fluctuation, produced by an OPO. The ZBD-induced off-resonance fluctuation and relative phase fluctuations can be estimated using the expression of $\epsilon \times \kappa$ and $\epsilon \times \pi$.

According to the full OPO equations of motion, the cavity length detuning will cause a shift of the squeezing angle, which can be expressed by [8]

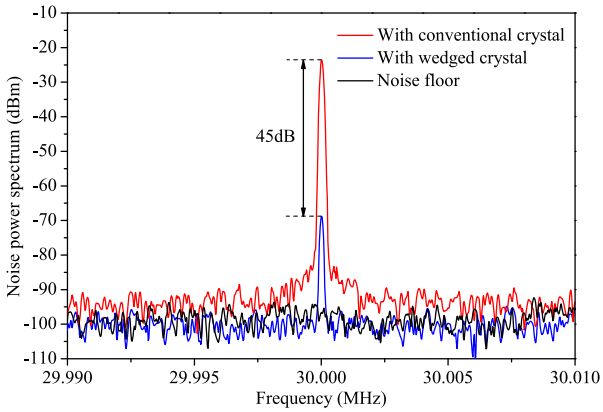

Fig. 3. Noise power spectrum of phase-modulated light at the modulation frequency.

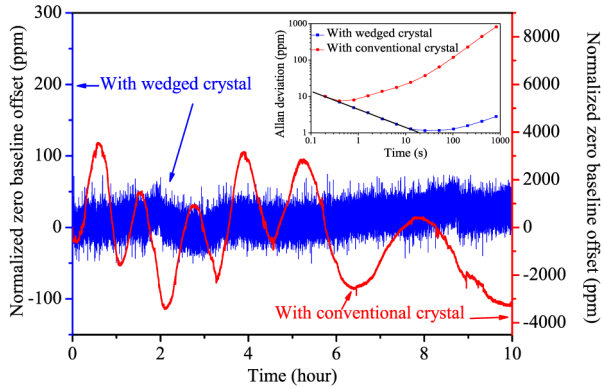

Fig. 4. Zero baseline offset normalized by the peak-to-peak value of the PDH error signal in 10 h. Left axis, normalized zero baseline offset with wedged crystal; right axis, normalized zero baseline offset with conventional crystal. Allan deviation associated with the zero baseline offset at the averaging time from 1 to 1000 s is shown in the inset.

$$\delta\theta_{\mathrm{squ}} = \frac{\epsilon \times \kappa}{\kappa(1+x^2)} \times \frac{180}{\pi}, \tag{1}$$

where κ is the half-width at half-maximum of the cavity transmission, and x is the gain factor $\sqrt{P/P_{\mathrm{th}}}$. When the gain factor x is 0.95, the squeezing angle fluctuation decreases from 0.1° to 0.002° under the conditions of the peak drift.

The relative phase between the pump and seed beams is locked at the most de-amplified (π) and amplified (0) phase to obtain quadrature amplitude and phase squeezed light, whose noise does also cause the squeezing angle fluctuations. The relative phase noise between the LO and squeezed beam would make the anti-squeezed quadrature contaminate the observed squeezing level. The relative phase noise originating from the ZBD of the PDH error signal, before and after using the wedged crystal, is reduced from 0.63° to 0.013°. Here we suppose there is a squeezed state generation system with the theoretical squeezing level of –10 dB. Considering all cavity length and relative phase fluctuations stemming from the ZBD, the quantum noise fluctuation is shown in Fig. 5. With the conventional modulation crystal, the observed squeezing is only –9.1 dB at worst, which shows that the

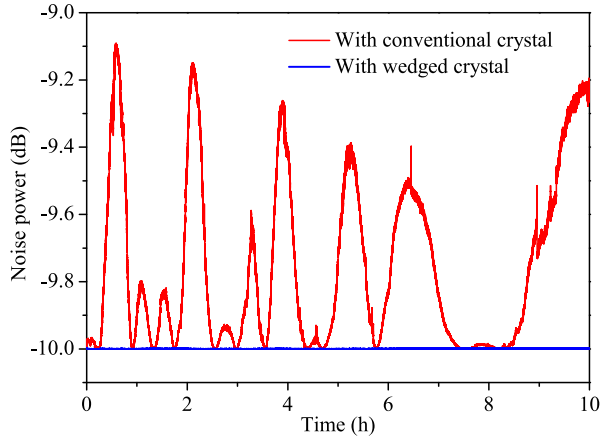

Fig. 5. Quantum noise fluctuation originating from the ZBD of the PDH error signal in 10 h.

fluctuation of the squeezing level is more than 0.9 dB in 10 h. However, with the wedged modulation crystal, the observed squeezing is −9.9998 dB at worst; the fluctuation of the squeezing level is less than 0.0002 dB in 10 h, without noticeable drift. The quantitative influence of the squeezing angle noise on the observed squeezing level is obtained from [9,11]. Obviously, the ZBD reduction can effectively improve the long-term stability performance of squeezed state generation system.

The inset of Fig. 4 shows the stability of the zero baseline offset described by Allan deviation. With the wedged crystal, the minimum Allan deviation is improved to 1.15 ppm at 13 s and clearly shows white noise dependence [20].

In conclusion, we have designed an EOM with a wedged MgO:$LiNbO_3$ crystal as the modulation crystal. According to the natural birefringence, the wedged design differentiates the deflection angles of the ordinary and extraordinary waves, two polarization components are completely separated in space, and the interference between the carrier and two orthogonal sidebands is eliminated. The RAM and the ZBD of the PDH error signal originating from the polarization misalignment and the etalon effect is reduced. Compared with the conventional EOM, the noise power spectrum of phase-modulated light with the wedged EOM is suppressed from −24 to −69 dBm; the peak-to-peak ZBD associated with RAM in 10 h is reduced from +3500/−3400 ppm to +70/−50 ppm. The influence of the ZBD of error signal on quantum noise fluctuation is effectively reduced. Most important of all, there is unnecessary to use some additional servo controls, and align carefully the polarization of the input beam, which greatly simplifies the alignment process and the setup of squeezed state generation.

Funding. National Natural Science Foundation of China (NSFC) (11504220, 61575114); Program for Outstanding Innovative Teams of Higher Learning Institutions of Shanxi; Program for Sanjin Scholars of Shanxi Province.

REFERENCES

1. K. Goda, O. Miyakawa, E. E. Mikhailov, S. Saraf, R. Adhikari, K. Mchenzie, R. Ward, S. Vass, A. J. Weinstein, and N. Mavalvala, Nat. Phys. **4**, 472 (2008).
2. H. Grote, K. Danzmann, K. L. Dooley, R. Schnabel, J. Slutsky, and H. Vahlbruch, Phys. Rev. Lett. **110**, 181101 (2013).
3. S. L. Braunstein and P. van Loock, Rev. Mod. Phys. **77**, 513 (2005).
4. A. Furusawa, J. L. Sorensen, S. L. Braunstein, C. A. Fuchs, J. J. Kimble, and E. S. Polzik, Science **282**, 706 (1998).
5. H. Vahlbruch, M. Mehmet, S. Chelkowski, and R. Schnable, Phys. Rev. Lett. **100**, 033602 (2008).
6. T. Eberle, S. Steinlechner, J. Bauchrowitz, V. Haendchen, H. Vahlbruch, M. Mehmet, H. Ebhardt, and R. Schnabel, Phys. Rev. Lett. **104**, 251102 (2010).
7. H. X. Chen and J. Zhang, Phys. Rev. A **79**, 063826 (2009).
8. S. Dwyer, L. Barsotti, S. S. Y. Chua, M. Evans, M. Factourovich, D. Gustafson, T. Isogai, K. Kawabe, A. Khalaidovski, P. K. Lam, M. Landry, N. Mavalvala, D. E. McClelland, G. D. Meadors, C. M. Mow-Lowry, R. Schnabel, R. M. S. Schofield, N. Smith-Lefebvre, M. Stefszky, C. Vorvick, and D. Sigg, Opt. Express **21**, 19047 (2013).
9. T. C. Zhang, K. W. Goh, C. W. Chou, P. Lodahl, and H. J. Kimble, Phys. Rev. A **67**, 033802 (2003).
10. T. Tanimura, D. Akamatsu, Y. Yokoi, A. Furusawa, and M. Kozuma, Opt. Lett. **31**, 2344 (2006).
11. Y. Takeno, M. Yukawa, H. Yonezawa, and A. Furusawa, Opt. Express **15**, 4321 (2007).
12. Y. Wang, H. Shen, X. L. Jin, X. L. Su, C. D. Xie, and K. C. Peng, Opt. Express **18**, 6149 (2010).
13. E. A. Whittaker, M. Gehrtz, and G. C. Bjorklund, J. Opt. Soc. Am. B **2**, 1320 (1985).
14. J. Sathian and E. Jaatinen, Appl. Opt. **51**, 3684 (2012).
15. I. Silander, P. Ehlers, J. Y. Wang, and O. Axner, J. Opt. Soc. Am. B **29**, 916 (2012).
16. R. W. P. Drever, J. L. Hall, F. B. Kowalski, J. Hougu, G. M. Ford, A. J. Munley, and H. Ward, Appl. Phys. B **31**, 97 (1983).
17. N. C. Wong and J. L. Hall, J. Opt. Soc. Am. B **2**, 1527 (1985).
18. W. Zhang, M. J. Martin, C. Benko, J. L. Hall, J. Ye, C. Hagemann, T. Legero, U. Sterr, F. Riehle, G. D. Cole, and M. Aspelmeyer, Opt. Lett. **39**, 1980 (2014).
19. L. F. Li, F. Liu, C. Wang, and L. S. Chen, Rev. Sci. Instrum. **83**, 043111 (2012).
20. W. G. Ma, Z. X. Li, W. Tan, G. Zhao, X. F. Fu, L. Zhang, L. Dong, W. B. Yin, and S. T. Jia, Appl. Phys. Express **6**, 112501 (2013).
21. T. Kessler, C. Hagemann, C. Grebing, T. Legero, U. Sterr, F. Riehle, M. J. Martin, L. Chen, and J. Ye, Nat. Photonics **6**, 687 (2012).
22. L. F. Li, H. Shen, J. Bi, C. Wang, S. S. Lv, and L. S. Chen, Appl. Phys. B **117**, 1025 (2014).
23. Z. X. Li, L. H. Zhao, W. Tan, W. G. Ma, G. Zhao, X. F. Fu, L. Dong, L. Zhang, W. B. Yin, and S. T. Jia, Sens. Actuators B **196**, 23 (2014).
24. K. Kokeyama, K. Izumi, W. Korth, N. Smith-Lffebvre, K. Arai, and R. Adhikari, J. Opt. Soc. Am. A **31**, 81 (2014).
25. J. Sathian and E. Jaatinen, J. Opt. **15**, 125713 (2013).
26. M. Gehrtz, G. Bjorklund, and E. Whittaker, J. Opt. Soc. Am. B **2**, 1510 (1985).
27. Y. H. Zheng, F. Q. Li, Y. J. Wang, K. S. Zhang, and K. C. Peng, Opt. Commun **283**, 309 (2010).
28. Y. J. Wang, Y. H. Zheng, C. D. Xie, and K. C. Peng, IEEE J. Quantum Electron. **47**, 1006 (2011).
29. H. D. Lu, J. Su, Y. H. Zheng, and K. C. Peng, Opt. Lett. **39**, 1117 (2014).